

PERFORMANCE OF A NEW COAXIAL HIGHER-ORDER-MODE DAMPER

DAVID JOFFE and AMIYA MITRA

TRIUMF, 4004 Wesbrook Mall, Vancouver, B.C., Canada V6T 2A3

(Received 9 May 1995; in final form 14 July 1995)

A new type of rf damper, designed to suppress higher-order modes which may excite beam instabilities, was built and tested on a ferrite-tuned coaxial cavity proposed for use in the KAON Factory at TRIUMF. The damper consisted of a series of rod and disc structures arranged at the open end of the cavity around the beam axis to form the capacitances and inductances of a multi-element Chebyshev high-pass filter. The damper was tested on the cavity and found to significantly damp all higher-order TEM modes with minimal effect at the fundamental frequency. A second version of the damper was also built and attached to a simple coaxial $\lambda/4$ cavity on which cavity perturbation bead-pull measurements were made. These showed that the damper significantly reduced the shunt impedance of TEM higher-order-modes while leaving the shunt impedance of the system at the fundamental frequency intact.

KEY WORDS: Impedances, radio-frequency devices

1 INTRODUCTION

Accelerating cavities require adequate damping of higher-order modes in order to avoid exciting multibunch instabilities. The strength of these modes can be characterized using the concept of shunt impedance: the impedance measured along the beam path across the cavity gap for any given frequency. Many types of structure have been designed to damp the energy of the higher-order modes (HOMs) and reduce these higher frequency impedances. Unfortunately, while many HOM damper designs may do this quite successfully, many also absorb significant amounts of energy from the cavity at the fundamental mode as well, the mode in which energy is transferred to the beam. Thus the overall rf efficiency of the cavity may be reduced in the attempt to damp potentially destructive higher-order modes at specific fixed frequencies. The situation becomes even more complicated when one attempts to damp higher-order modes in cavities meant to operate over a sizable range of frequencies, such as the ferrite-tuned cavity designed for the proposed KAON Factory Booster Ring at TRIUMF.^{1,2}

In light of this problem, a new design for a HOM damper has been developed at TRIUMF which would both preserve cavity rf efficiency, and be effective at all frequencies above a certain cut-off point. This new damper acts as a multi-element high-pass filter, absorbing all energy from fields above the corner frequency of the filter, while leaving the fields at the

fundamental frequency as undisturbed as possible. To test the effectiveness of this new type of damper it was necessary to measure the shunt impedance of the combined cavity/damper system at both the fundamental frequency and at the frequency of the higher-order modes.

2 DESIGN CONCEPT OF COAXIAL HOM DAMPER

The design aim is to find a damper which will provide a low shunt impedance (below $1 \text{ k}\Omega$) for all the higher-order modes, but retain a high shunt impedance for the fundamental accelerating mode. The damper should demonstrate the above performance as the frequency of the fundamental mode swings through its entire range; 46 to 61 MHz in the case of the ferrite-tuned cavity proposed for the KAON Factory. Thus the damper is required to be a broad-band device, damping all the higher-order modes related to the sweeping fundamental frequency. It must have the effect of a high-pass filter with a sharp cut-off characteristic. The HOM damper should also be designed to withstand an accelerating gap voltage of 60 kV for the proposed cavity.^{3,4}

If a high-pass filter is terminated with a resistive load and attached to the gap of an accelerating cavity with its cut-off frequency chosen to provide adequate attenuation for the fundamental currents but none for the HOMs, then such a device would be ideally suitable as a HOM damper. The high-pass filter described in this paper has been designed particularly for the KAON Booster cavity operating from 46 to 61 MHz, for which the first higher-order mode is the third harmonic ranging from approximately 140 to 180 MHz. Thus a five element Chebyshev high-pass filter has been chosen with a cut-off frequency of 140 MHz providing more than 40 dB attenuation at the fundamental with better than 0.1 dB ripple.⁵

The filter specifications can be summarized as follows:

Number of elements	5
High-pass cutoff frequency	140 MHz
Minimum attenuation at 61 MHz	40 dB
Maximum pass-band ripple up to 1 GHz	1 dB
Maximum source impedance	1Ω
Load impedance	50Ω

Figure 1 shows the element values for such a filter and the computed frequency response.

A prototype of the higher-order mode damper described above was constructed which could be attached to the open end of a coaxial quarter-wavelength test cavity, as shown in Figure 2.⁶ The length of the test cavity was adjusted to provide a fundamental resonant frequency of 70 MHz. The inner diameter of the outer conductor of the quarter-wavelength cavity was 6 in. and hence the prototype HOM damper was constructed with the same outer dimension of 6 in. Realization of the high-pass filter in coaxial form mounted at the gap of the accelerating cavity was effected in the following way. The capacitances C2 and C3 were provided by the gaps between three hollow discs which were connected to the short-circuited (end) plate by four rods which provided the inductances L1 and L2.

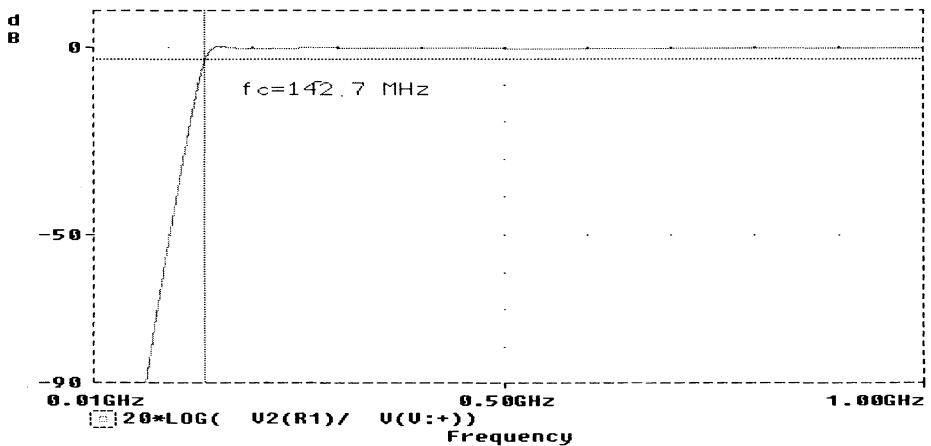
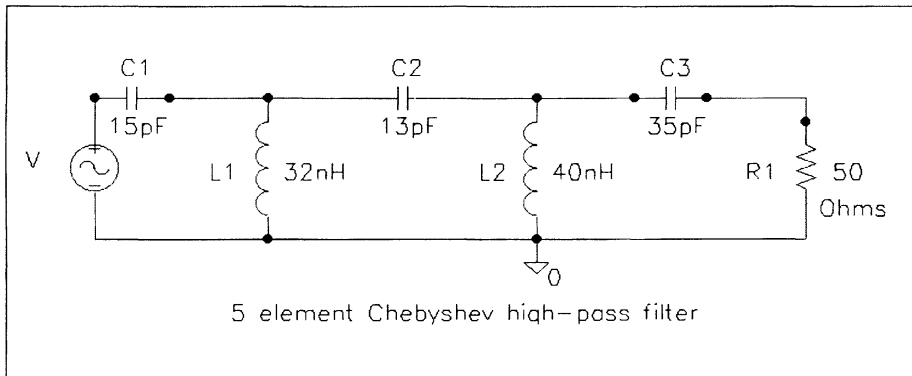


FIGURE 1: Schematic and computed filter response of a five-element high-pass filter.

The discs and the rods were mounted so as to allow the passage of beam through the filter-cavity structure. The capacitance $C1$ was that between the open end of the inner conductor of the accelerating cavity and first disc of the filter. Four 50Ω loads were mounted on the damper and were connected to the third disc by low-inductance straps.

The above filter structure constitutes a three-gap structure, thus adding another set of modes to the cavity which can be excited by a passing beam. By introducing a horn, which was equivalent to a series capacitance and a shunt inductance, between the cavity gap and the first filter disc, it was hoped that the coupling of beam current to the filter resonances could be minimized. The horn restored the single-gap structure of the cavity by shielding the filter from the beam, and provided a higher attenuation for the principal mode by modifying the filter structure from a 5-element to a 7-element one.

The excellent damping performance of the 6 in. model led to the design of a full scale HOM damper for the KAON Booster cavity. Figure 3 shows the cross sectional view of the

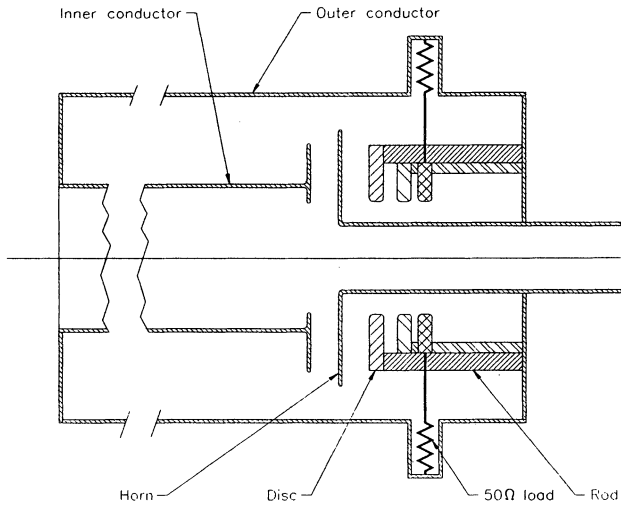


FIGURE 2: 6 in. test cavity and higher-order-mode damper.

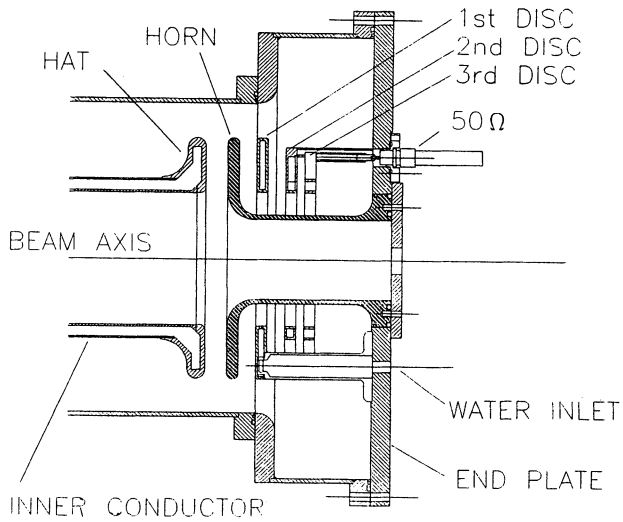


FIGURE 3: Ferrite-tuned cavity and full-scale higher-order-mode damper.

coaxial filter and part of the accelerating cavity. The high voltages between the capacitor plates (maximum 60 kV) and water cooling of the various components of the filter were some of the design considerations for this full scale HOM damper. As in the 6 in. model, the capacitances of the filter were formed out of the gaps between a set of hollow coaxial discs and the inductors were made from hollow rods connected between the end plate and their respective capacitive discs. This made the filter components self-supporting without the use of any dielectric or potentially lossy material. All material used for the filter was either copper or copper-clad. The inductive rods which supported the capacitive discs were used for water inlet and outlet for cooling both the inductors and the capacitors. The final disc in the filter structure was supported by four rods connecting to four water cooled 50 ohm terminating loads. The four rods which formed the inductors were welded to the end plate after the gaps between discs and the lengths of the inductive rods had been optimized for the best filter performance.

The horn was made from a hollow tube concentric with the beam axis with a disc of the same diameter as the inner conductor "hat" welded to it. In order to obtain the required capacitance between the cavity and the first element of the filter a hat was added to the inner conductor also.

3 SHUNT IMPEDANCE AND PERTURBATION THEORY

In order to evaluate the performance of the higher-order-mode damper, a method is required for measuring the shunt impedance, defined as the ratio of the voltage across a given gap to the resistive current. This quantity can be found by using the geometry and properties of the resonating structure alone, independent of the properties of the beam current. In the case of resonant frequencies of the system this quantity can be calculated directly as the square of the peak voltage V seen by the beam across the gap divided by twice the input power P .

$$R_s = V^2/2P \quad (1)$$

Any mode which can exist in the cavity could potentially be excited by the beam, and thus one would like to know the value of the impedances for all the resonating modes of the cavity.

There are various methods which one can use to determine the shunt impedance without having to measure absolute power levels or gap voltages. Some of these require conducting probes which run fully across the cavity gap, thus seriously altering the field patterns inside the cavity and giving potentially spurious results, particularly at higher frequencies.⁷ Cavity perturbation measurements avoid such problems by using as the probe a small spherical dielectric bead which alters the fields inside the cavity in a regular and calculable way.^{8,9} When these beads are placed in the electric field of a resonating structure, the frequency of the resonance will be pulled down by an amount directly related to the strength of the original field at that location.

The strength of the field can be determined from the following formula:^{10,11}

$$E^2 = \frac{QP\delta\omega}{\pi\epsilon^*r^3\omega} \quad (2)$$

Here E is the magnitude of the electric field, $\delta\omega$ is the frequency shift caused by the bead, Q is the quality factor of the resonance, P is the power going into the cavity, ω is the frequency of the resonance, r is the radius of the bead, and ε^* is the modified dielectric constant which is related to the dielectric constant ε of the bead by the relation:

$$\varepsilon^* = \frac{\varepsilon_0(\varepsilon - \varepsilon_0)}{\varepsilon + 2\varepsilon_0} \quad (3)$$

The shunt impedance is defined in Equation (1) as the ratio of the gap voltage squared to the input power. If we expand the voltage term as the integral of the electric field across the gap a situation where the electric field is known to be parallel to the ion path (such as along the axis of the coaxial $\lambda/4$ resonator for TEM modes) then we may substitute for \mathbf{E} using Equation (2), with the result:

$$R_S = \frac{Q \left[\int_P (\delta\omega)^{1/2} dz \right]^2}{2\pi \varepsilon^* \omega^2 r} \quad (4)$$

We now have an expression for the shunt impedance which depends only on the physical and electrical properties of the bead, the frequency and frequency shift of the cavity, the Q factor of the cavity, and the length of the path. To make the integral a measurable quantity one can replace it with a sum over a series of n steps along the path with each step having length Δz , which will depend on the detail required for the field profile.

The above relations for finding the shunt impedance of a cavity rest on a few assumptions which must be valid for the measurements to be accurate. In the first place the bead must be small enough that its volume is minuscule compared to the total volume of the cavity and that the unperturbed field is more or less uniform over the volume of the sphere; for rapidly varying field patterns smaller beads will be necessary. Also the bead must be at least one diameter away from any conducting cavity wall or edge in order to minimize additional effects caused by images of the bead in the conductor. Finally, Equation (4) for determining the shunt impedance assumes that the direction along which the bead is being pulled is parallel to the direction of the electric field.

4 MEASUREMENT OF SHUNT IMPEDANCE

4.1 Measurement devices

The apparatus used for making cavity perturbation measurements consisted of several parts, an overall schematic of which appears in Figure 4. The test cavity on which the measurements were performed was a 6 in. coaxial $\lambda/4$ resonator, to which the damper model which was being evaluated was attached, as described in Section 2. Beads made of Stycast ceramic (with a dielectric constant of 27.3 ± 0.1) were pulled through the cavity along a nylon line by an electric micro-stepping motor. This motor was driven by an indexer/controller which was itself controlled by an IBM 486 computer. This computer also controlled the Hewlett Packard 8753 network analyzer used to measure the properties of the cavity resonance. To the computer was also attached a printer to print out data as well

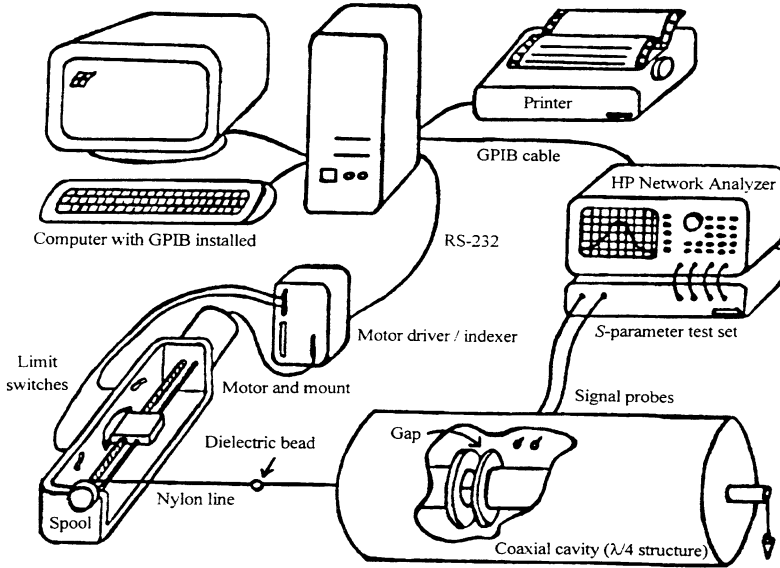


FIGURE 4: Perturbation measurement apparatus — overall scheme.

as storing it on disc as the measurements were made. The software used in the experiment contained some 40 pages of Quick Basic code developed during the course of the experiment to control all the various devices.¹¹

The apparatus was tested by measuring the shunt impedance of the test cavity at various resonant frequencies and comparing those values with the theoretical values for a quarter-wavelength coaxial resonator as well as the shunt impedance values measured using methods other than cavity perturbation.

For a coaxial quarter-wavelength transmission-line cavity, the theoretical shunt impedance for the TEM modes is given by:

$$R_S/Q = 4Z_0/n\pi \quad (5)$$

Here n is the number of the harmonic for each mode and Z_0 is the characteristic impedance of the transmission line as given by the formula:

$$Z_0 = (1/2\pi)(\mu_0/\epsilon_0)^{1/2} \ln(b/a) \quad (6)$$

where b and a are the radii of the outer and inner conductors respectively.

Equation (5) does not take into account the stored energy created by the capacitance of the end piece added to the outer conductor of the transmission line at the open end in order to form a gap which is parallel to the beam axis. This "tip capacitance" lowers the shunt

TABLE 1: R_S/Q of the test cavity as determined by a variety of methods.

Mode	f (MHz)	Q Factor	$R_S/Q(\Omega)$ from Eq.(7)	$R_S/Q(\Omega)$ $\partial\phi/\partial\omega$	$R_S/Q(\Omega)$ MAFIA	$R_S/Q(\Omega)$ Bead Pull
Fund.	71.4	2800	63.49	63.86	63.88	63.4±0.6
$n=3$	215.2	4812	21.16	21.45	21.85	21±1
$n=5$	358.9	5366	12.7	14.3	13.62	13±1
$n=7$	501.6	4422	9.07	11.29	10.29	10±1
$n=9$	645.2	1770	7.05	7.42	8.64	7±1

impedance by an amount which depends on the ratio of the length of the outer conductor to the length of the inner conductor ϕ . This lowered shunt impedance is given by:

$$\frac{R_S}{Q} = \frac{4Z_0 \sin_2((\pi/2)\phi)}{\pi\phi + \sin(\pi\phi)} \quad (7)$$

The theoretical values of the shunt impedance, including the tip capacitance effect, were calculated for the first five TEM modes, with the results recorded in Table 1.

Another method of determining the shunt impedance of the system involves connecting a conductor across the cavity gap and using the rate of change of phase of the reflected signal with frequency to calculate the shunt impedance according to the formula:

$$(\partial\phi/\partial\omega) \times R_S/Q = -4Z_0/\omega \quad (8)$$

This method was applied to the first five TEM modes of the cavity and the results are recorded in Table 1. Values of the shunt impedance calculated by a MAFIA (MAXwell's equations Finite Integration Algorithm) simulation are also recorded in Table 1. Finally, Table 1 shows the shunt impedance values of the five resonances as measured using the bead pull cavity perturbation apparatus.

4.2 Accuracy

The accuracy of the cavity perturbation technique in measuring shunt impedance was limited by a number of factors, the most important of which was the ability to measure small frequency shifts (on the order of a few kHz) in resonances with frequencies in the hundreds of MHz ranges. While the network analyzer used was capable of measuring such small shifts, the difficulty lay in separating out the frequency shift of the cavity caused by the perturbation with fluctuations in the resonant frequency caused by other factors (temperature change, mechanical vibration, etc.)

To compensate for these difficulties in measuring frequency shift the following measures were taken. The experiments were run at night in order to shield the cavity from the vibrations caused by the operation of heavy machinery in the area, as well as to minimize the temperature change in the room. An algorithm was written into the software which looked at the unperturbed frequency both before and after the bead pull was performed, and corrected

the perturbed frequency shift at each step for a linearly changing unperturbed frequency. Furthermore, the speed at which the apparatus performed the bead pull was increased to a rate of 2–3 seconds per step in order to minimize frequency fluctuations in the cavity and ensure that any changes in the frequency would be linear and thus hopefully compensated for by the software. The speed of the system was ultimately limited by the rate at which the network analyzer could sweep through a given set of frequencies — the system could only have been made faster by losing detail in each sweep. With the above adjustments made to the system, the frequency shifts in the cavity could be measured accurately down to the level of approximately 100 Hz. Several measurements were taken at each frequency, and the results examined. The strongest resonances (particularly the fundamental frequency) could be measured to an accuracy of 1%. For some of the weaker higher-order mode resonances, the system could determine the shunt impedance to within 5–10%.

5 RESULTS OF MEASUREMENTS OF THE 6-INCH DAMPER AND CAVITY

5.1 *Higher-order modes*

The 6-inch higher-order-mode damper structure was attached to the open end of the quarter-wavelength coaxial test cavity. Measurements were taken both with and without the horn structure attached in order to observe its effect on the shunt impedance of the overall system.

The combined cavity/damper structure had a fundamental resonant frequency of 65.5 MHz with the horn, a much lower frequency than the value of ~ 70 MHz for the cavity without the damper structure. This 4 MHz reduction in the overall fundamental frequency is due primarily to the heavy capacitive tip loading of the damper structure. For the damper without the horn, the tip loading was not quite as large and the fundamental frequency was found at 65.9 MHz. The harmonics of the fundamental TEM mode were also observed at frequencies which were slightly reduced due to tip loading. In contrast to the reduced frequencies of the TEM modes, the frequency of the circumferential mode ($TE_{1,1}$) at 714 MHz remained basically unchanged when the damper structure was added to the cavity.

The addition of the damper structure to the system not only altered the existing modes of the cavity, it also added two new sets of modes. The first set of new modes were those of the quarter-wavelength coaxial resonator made up of the damper itself, with the inner conductor terminating either on the horn or one of the disc structures. These modes occurred at frequencies of 600 MHz or higher. For this set of modes, the addition of the horn simply added one more resonance. The second set of modes introduced were those of the half-wavelength coaxial resonator made up of the combined test cavity and damper structure. In this case the inner conductors of the damper and cavity act as a single inner conductor broken by a capacitance across the gap. These half-wavelength resonances were much stronger with the horn in place, when the capacitance across the gap was larger. They were also stronger for higher frequency harmonics, since for these the capacitance appears more like a short circuit across the gap in the inner conductor, and the system becomes a better half-wavelength resonator. These resonances were observed starting around 255 MHz with the horn attached, and around 500 MHz with the damper alone, since in this case the lower frequency mode was too faint to detect.

TABLE 2: Effect of HOM damper with the horn attached.

Frequency (MHz)	Unloaded Q Factor	Unloaded R_S k(Ω)	Loaded Q Factor	Loaded R_S k(Ω)
65.4940±0.0001	2423±2	157±1	2341.4±0.4	148±1
195.692±0.002	2000±10	33±3	63.31±0.02	<1
255.547±0.001	1260±5	3.0±0.3	9.135±0.005	<0.02
339.629±0.003	1674±4	6.2±0.6	No resonance observed	No resonance observed
416.650±0.001	1259.2±0.4	1.9±0.2	9.6±0.2	<0.01
520.5281±0.0006	3168±5	0.22±0.02	45.4±0.1	<0.003
644.19±0.02	407±3	<0.1	No resonance observed	No resonance observed
656.849±0.009	657±1	<0.05	No resonance observed	No resonance observed
661.123±0.004	1281.7±0.3	<2	40.2±0.1	<0.06
714.295±0.007	724±3	<0.7	303.9±0.1	<0.3

TABLE 3: Effect of HOM damper with no horn.

Frequency (MHz)	Unloaded Q Factor	Unloaded R_S k(Ω)	Loaded Q Factor	Loaded R_S k(Ω)
65.8665±0.0004	2041±3	96±2	2036±3	94±4
204.984±0.001	1759±6	32±3	38±1	<0.7
327.999±0.003	1182±1	7.3±0.7	6.8±0.1	<0.04
413.638±0.006	1150±20	1.0±0.7	39.0±0.2	<0.03
515.328±0.002	2210±1	<2	No resonance observed	No resonance observed
571.63±0.05	1400±100	<6	No resonance observed	No resonance observed
640.60±0.04	228±7	<1	No resonance observed	No resonance observed
653.965±0.004	864.8±0.8	<0.5	38.45±0.03	<0.01
713.94±0.04	619±3	<2	300.4±0.1	<1

For both of these new types of modes, the shunt impedances were much lower than that of the fundamental resonance. The largest shunt impedance of one of the new modes was 3 k Ω , less than 2% of the impedance at the fundamental. All the new modes were damped strongly once the damper was fully loaded, and in no case did the new modes have impedances which exceeded 100 Ω when all four loads were attached. This is significant since it means that the addition of the damper structure did not add any modes for which the shunt impedance across the gap would be greater than 1 k Ω in the fully damped system, and thus potentially result in serious beam instabilities. It is also worth noting that the addition of the damper structure did not add any new circumferential modes in the relevant frequency range (up to 800 MHz).

5.2 Shunt Impedances

With the higher-order-mode damper structure attached to the cavity the frequency, Q factor, and shunt impedance of each mode (up to 800 MHz) was measured using the bead-pull apparatus, with and without the horn, and with and without all four loads attached. The results obtained with the horn attached are given in Table 2, those obtained without the horn attached are given in Table 3. Note that the frequencies given in the tables are those of the various modes with no loads attached.

The damper was effective in damping the higher-order-mode resonances without strongly affecting the fundamental resonance both with and without the horn attached. At the fundamental frequency, the measured reduction in Q factor as a result of damping (which is a measure of the power lost) was 3% for the damper with the horn attached, and 0.3% for the damper with no horn attached. Although this would seem to indicate that the filter without the horn gives a better performance at the fundamental frequency, the power lost by the filter with the horn could probably have been reduced by optimizing the capacitances between the horn and the inner conductor and the horn and the first disc. The shunt impedances also remained relatively unchanged at the fundamental frequency, with the damper reducing the fundamental impedance by 6% with the horn attached, and by 2% with no horn.

At the higher-order TEM modes up to 800 MHz both damper designs were effectively able to damp both the Q factors and shunt impedances. The Q factors of these modes were damped between 95% and 100% both with and without the horn, and in all cases the HOM shunt impedances were brought below 1 k Ω .

With the horn attached the damper became effectively a seven- rather than a five-element filter. Although the seven-element filter gave sharper attenuation below the corner frequency, above it the response of both filters was essentially the same. Thus the presence of the horn makes very little difference to the capacity of the damper for the higher-order TEM modes. The damper had a much less dramatic effect on the non-TEM modes to which the high-pass filter was less able to couple effectively. For the $TE_{1,1}$ mode found at 714 MHz the damper reduced the Q -factor of the resonance by approximately 50% (see Tables 2 and 3), bringing the shunt impedance to below 1 k Ω both with and without the horn.

Although adding the horn to the cavity did not significantly change the performance of the damper, it did cause one specific change in the pattern of the field across the gap. Figure 5 shows the frequency shift (which is proportional to the square of the electric field strength) as the bead was pulled across the gap both with the horn attached and without. Although the gap between the inner conductor and the first damper element was set to the same value for both configurations, the effective total gap of the cavity/damper structure with no horn attached was larger, so that the discs were inside the overall gap rather than beyond it. The change in the field pattern caused by removing the horn was to distribute the field along the entire length of this new extended gap, while keeping the shunt impedance more or less constant.

6 HIGH POWER TEST OF THE HOM DAMPER

The full-scale HOM damper with the horn attached, as shown in Figure 3, was installed on the ferrite-tuned Booster cavity. Prior to the high power test, an attempt was made to

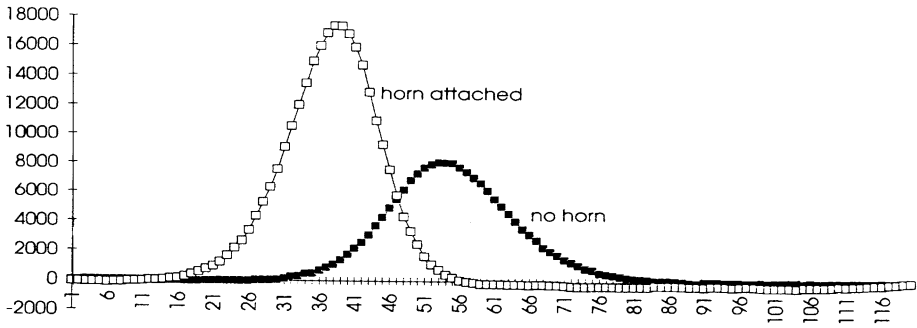


FIGURE 5: Field profile along damper/cavity axis with and without horn attached.

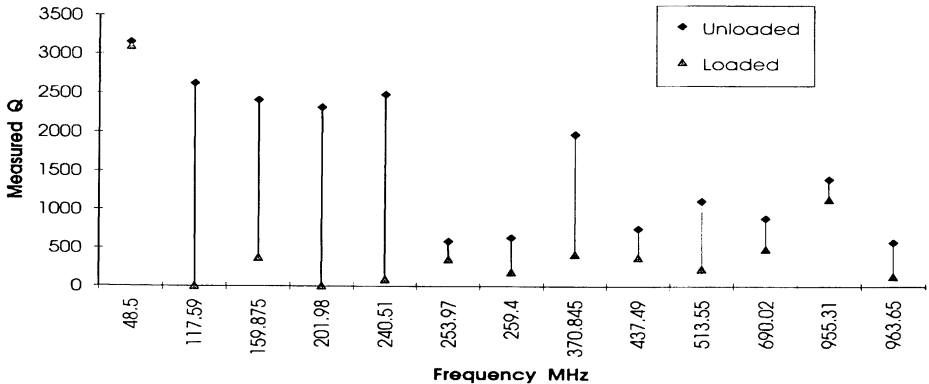


FIGURE 6: Q measurement of the ferrite tuned cavity with damper installed and horn attached.

estimate the shunt impedance of the damper-cavity system using the perturbation technique. Since the resonant frequency of the ferrite-tuned cavity was governed by the bias current, the stability of this current dictated the stability of the resonant frequency. Unfortunately, the shift in the resonant frequency due to bias current variation was more than an order of magnitude greater than the frequency shift expected from perturbation measurements, hence shunt impedance measurements of the combined damper-cavity configuration could not be carried out by the perturbation technique. However, the Q factors and shunt impedances of the resonances or higher-order modes of the damper alone were measured and are shown in Table 4. The Q factors of all the higher-order modes were significantly damped when the damper was terminated with 50Ω loads, with the exception of a circumferential ($TE_{1,1}$) mode at 460 MHz. The undamped and damped Q factors of the cavity-damper configuration are shown in Figure 6.

A hat was added to the inner conductor of the ferrite-tuned cavity at the gap end to help form the first capacitance of 15 pF of the filter. The gap between the cavity inner conductor

TABLE 4: Resonances of the full-scale higher-order-mode damper with horn attached.

Frequency (MHz)	Unloaded Q -factor	Unloaded R_S (k Ω)	Loaded Q -factor	Loaded R_S (k Ω)
205	2000	23.9	10	0.1
440	1000	1.3	240	0.3
460	1100	5.2	940	4.4
503	1750	0.3	75	0.1
601	1900	0.3	<5	<0.01
738	1500	1.4	300	0.3

and the horn was set to a value of 20 mm. The cavity with the damper installed was rf conditioned under a vacuum of 1.2×10^{-6} Torr. The cavity resonant frequency was set to 47.8 MHz with a dc bias current of 1320 A on the ferrite tuner. A voltage of 60 kV could be maintained at the accelerating gap of 20 mm under cw operating condition at the above rf operating frequency. The gap voltage was calibrated using x-ray measurement. Under low-duty-cycle pulse operation, a voltage of 80 kV at the gap could be achieved without any breakdown. The power absorbed at one of the four 50 Ω terminating loads with a gap voltage of 63 kV was measured to be only 11 W.

Similar measurements at the fundamental frequency of the cavity were carried out with the horn removed from the damper. The gap between the first capacitive disc of the filter structure and the hat mounted on the inner conductor of the cavity was also kept at 20 mm. Without the horn the damper coupled 2 dB more power at the fundamental frequency than the damper with the horn, as can be seen from Figure 7. The gap voltage was kept at 60 kV under low-duty-cycle pulsing instead of in cw mode, due to time constraints.

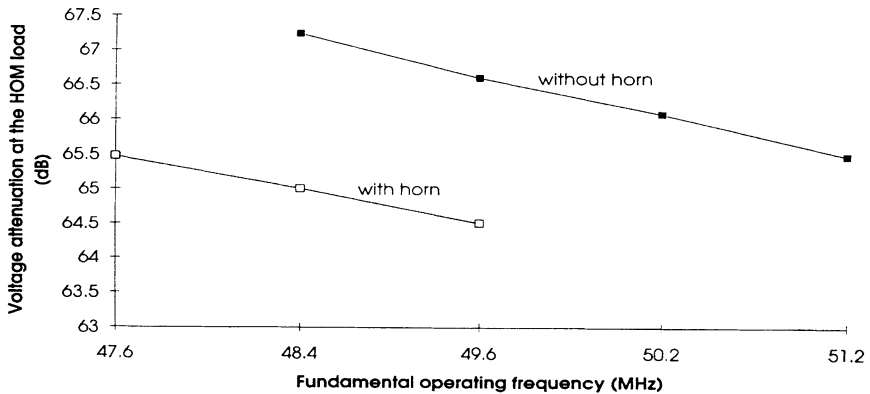


FIGURE 7: Damper coupling to the fundamental frequency with and without horn attached.

7 DISCUSSION

Accurate knowledge of the shunt impedance of this type of filter structure when attached to the resonant cavity is of the utmost importance in predicting its usefulness as a higher-order-mode damper. Emphasis was given to measuring shunt impedances, as opposed to simply the Q -factor of the resonance, in determining damper performance, and the perturbation measurement outlined in section 3 proved to be the most accurate and effective method of determining these impedances. Perturbation measurements of the shunt impedances of the combined cavity/damper system compared well with results obtained from MAFIA simulations run on the same system.¹²

Some conclusions may be drawn from the measurements described in sections 5 and 6. The damper is seen to be effective up to the 800 MHz range both with and without the horn attachment, meaning that the horn may not be entirely necessary to shield the multiple gap structure from the beam. The higher-order modes which were least affected by the damper (damped by only 50% when the loads were attached) were the circumferential modes of the structure itself, which tended to limit the pass band of the filter. It should be possible to suppress these circumferential modes by cutting radial slots on the discs or cutting the discs into halves (this option makes the design of water cooling difficult). To improve the filter performance further, we would like to examine the upper limit of the pass-band. This limit corresponds roughly to the frequency at which the rods act as quarter-wavelength resonators; beyond this frequency the rods no longer behave as proper inductors in the filter circuit and reducing the lengths of these inductors would increase the pass-band limit. For the full scale HOM damper the $\lambda/4$ resonances of the inductors loaded by their respective capacitive discs were close to 700 MHz. Furthermore, the rods that connect the last disc to the 50Ω terminating loads should be as non-inductive as possible, so it would be advantageous to minimize the lengths of these final connecting rods. There is also room for further optimization of the filter components with respect to the lower pass-band ripple of the filter.

8 CONCLUSION

Both signal-level and high-power tests show that this new type of coaxial filter performs well as a higher-order-mode damper. The horn version is theoretically slightly more attractive since given the same corner frequency the filter can be designed to couple even less power at the fundamental. However, the measured voltage attenuation of 65 dB at 48.3 MHz is more than satisfactory even without the horn. This type of damper does not suffer from excessive coupling of power at the fundamental frequency as is evident from the measured loss of Q of only 4% at 48.3 MHz with the damper attached.

This kind of higher-order-mode damper employing a high-pass filter in a coaxial form is very suitable for single gap cavities similar to the one described in this paper; being coaxial, it becomes an integral part of the resonant cavity. The same damper can be mounted outside the cavity if adequate capacitive coupling to the beam gap can be achieved.

ACKNOWLEDGEMENTS

The authors would like to thank Michael Craddock for his invaluable support, and Roger Poirier for his insight and discussion on the damper and cavity system. Also, they would like to thank Peter Harmer for his assistance in Autocad drawing and fabrication.

REFERENCES

1. M.K. Craddock, "The Status of the KAON Project," *ICFA Seminar on Perspectives in High Energy Physics*, DESY, 1993.
2. *KAON Factory Proposal*, (ed.) M. Craddock, "Accelerator System", Chapter 4, TRIUMF, 1985.
3. T. Enegren, R. Poirier, *et al.*, "Higher Order Mode Damping in KAON Factory RF Cavities", *Proc. of the 1989 IEEE Particle Accelerator Conf.*, **1**, 196–198 (1989).
4. W.R. Smythe, T.A. Enegren and R.L. Poirier, "A Versatile RF Cavity Mode Damper," *Proc. of the 2nd European Particle Accelerator Conf.*, **1**, 976–978 (1990).
5. A.K. Mitra, "Higher Order Mode Dampers for the KAON Booster Cavity," *Proc. of the 1993 Particle Accelerator Conf.*, **2**, 974–976, (1993).
6. A.K. Mitra, "A New Concept of a Higher-Order-Mode Damper for the KAON Booster Cavity," *Proc. of the 4th European Particle Accelerator Conf.*, **3**, 2158–2160, (1994).
7. T.A. Enegren, "Measurement of RF Shunt Impedance", TRIUMF, Design Note, 89-K104, 1989.
8. H. Klein, N. Merz, *et al.*, "Field Distribution, Power Losses and Parameter Optimization of Helical Accelerator Structures", *Particle Accelerators*, **3**, 235–244, (1972).
9. H. Klein, "Basic Concepts I", *Proc. of the 1991 CERN Accelerator School*, **1**, 97–124, (1991).
10. S.W. Kitchen and A.D. Schelberg, "Resonant Cavity Field Measurements", *Journal of Applied Physics*, **26**, 5, 618–621, (1954).
11. D. Joffe, "Cavity Perturbation Measurements of the Shunt Impedance of a Tuned Resonator with Higher-Order-Mode Damping", M.Sc. Thesis, University of British Columbia, 1994.
12. E. Zaplatin, "Studies of the TRIUMF KAON Factory Booster Cavity HOM Damper", *Proc. of the 4th European Particle Accelerator Conf.*, **3**, 2161–2163 (1994).